

PAGER-M: A Novel Location-based Routing Protocol for Mobile Sensor Networks

Le Zou, Mi Lu, Zixiang Xiong

Department of Electrical Engineering, Texas A&M University
lezou@ee.tamu.edu, mlu@ee.tamu.edu, zx@lenna.tamu.edu

Abstract

In this paper we present a location-based routing protocol called Partial-partition Avoiding Geographic Routing-Mobile (PAGER-M), for mobile sensor networks that consist of frequently moving sensors. The protocol uses the location information of sensors and the base station to assign a cost function to each sensor node, which is close to the Euclidean length of a sensor node's shortest path to the base station. A packet is forwarded to the base station using greedy forwarding whenever possible. When a packet reaches sensor nodes near local minimums, where greedy forwarding will be impossible after a number of hops, the packet is forwarded following the high-cost-to-low-cost rule. Extensive simulations are used to compare the performance of PAGER-M with Greedy Perimeter Stateless Routing (GPSR) and Ad-hoc On-demand Distance Vector protocol (AODV) in mobile sensor networks. Experimental results show that PAGER-M achieves higher delivery ratio, lower routing overhead and lower energy consumption.

1. Introduction

Wireless sensor networks [1] consist of a large number of densely deployed sensors that have wireless communication, computing, and sensing capacities. In some application scenarios, sensor nodes in these networks move frequently either because they have locomotion capacity or because of the instability of the sensing environment. These mobile sensor networks find applications ranging from biology or biocomplexity research [2], search-and-rescue operations, and environment monitoring [3]. They require efficient and reliable routing protocols rather than *flooding* when the network mobility is not too high to make it the only choice.

Many routing protocols [4~20] have been proposed for ad-hoc/sensor networks. Among them, a number of location-based routing protocols [14~20] have been studied. These location-based protocols utilize the location information of sensor nodes to achieve scalability [21] in large-scale sensor networks.

Location service systems [22~24] also justify the use of these location-based routing protocols. Among them, stateless routing protocols do not require a node to memorize past traffic/paths, thus maintain almost no state information. Greedy-Face-Greedy (GFG) [17] and Greedy Perimeter Stateless Routing (GPSR) [18] are currently the most popular stateless location-based routing methods in mobile wireless ad-hoc/sensor networks. GFG/GPSR is shown to perform well in considerably dense (average degree > 20) wireless networks with dynamic topologies. However, as shown in this paper, when the density of wireless networks is reduced, the performance of GPSR also begins to decrease.

In this paper, we propose a novel location-based routing protocol called PAGER-M for mobile wireless sensor networks. PAGER-M utilizes the location information of sensor nodes and the base station to assign each sensor node a *cost*, which is close to a sensor's Euclidean length of the shortest path to the base station. When a sensor node receives a packet, it forwards the packet to the base station using greedy forwarding [14] whenever possible. Greedy forwarding may fail at a *concave* node (local minimum) that has no closer neighbor to the base station. To avoid this situation, when a packet reaches sensor nodes near a concave node, the packet is forwarded to a neighbor following the high-cost-to-low-cost rule. PAGER-M does not require a node to memorize the past traffic/path; in this sense, it is a stateless location-based routing protocol. In PAGER-M, multiple forwarding choices are provided for a sending node. This path redundancy reduces the transmission failures caused by mobility. The beacon interval is randomized and prolonged to reduce the interference and routing overhead. Extensive simulations are used to compare the performance of PAGER-M with Greedy Perimeter Stateless Routing (GPSR) [18] and AODV [7] in mobile wireless sensor networks with different parameters. Experimental results show that PAGER-M has a higher delivery ratio, lower routing overhead and lower energy consumption.

We introduce our mobile sensor network model in section 2. After that, our routing scheme is described in section 3. In section 4, we explain optimization details in our protocol implementation. Experimental results are presented in section 5. Related works are compared with our protocol in section 6. In the end, we give our conclusion.

2. Mobile Sensor Network Model

We model a mobile sensor network as a unit graph with a base station. As Fig. 1 shows, a base station is adjacent to an unobstructed two-dimensional plane that consists a number of randomly deployed sensor nodes. The sensor nodes are modeled by a unit graph. All nodes within the communication range r of a node x are considered as neighbors of x and have bi-directional links with it. The base station has a communication range R , which is long enough to cover all sensor nodes. The sensor nodes can move randomly with random velocities on the sensing field. With mobility, each sensor node has different neighbors in and out of its communication range frequently as shown in Fig. 2.

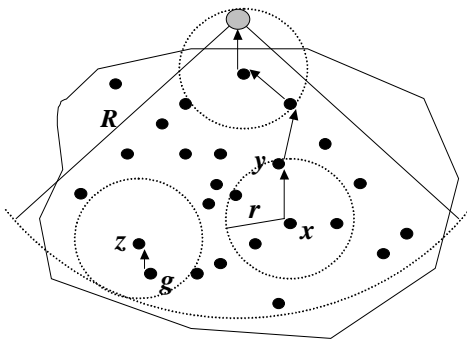


Fig. 1. The mobile sensor network model.

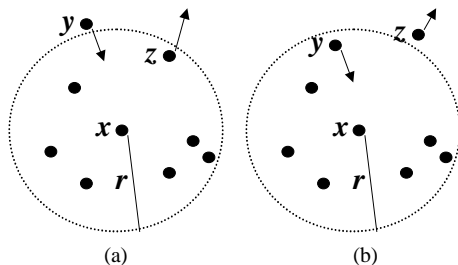


Fig. 2. A node has different neighbors at different moments due to mobility. (a) At t_0 , node x has node z as a neighbor that is moving out of its communication range. (b) At t_1 , node z has moved out of the communication range of node x , while node y has moved into the communication range of node x and become a new neighbor of x .

3. Distributed Routing Scheme

In this section we review greedy forwarding and introduce our cost-based forwarding methods before

discussing path redundancy provided by our protocol. Afterwards, we discuss the self-configuration property of PAGER-M.

3.1. Greedy Forwarding

In PAGER-M, information collected at a sensor node is forwarded to the base station in a multi-hop manner using greedy forwarding [14] whenever possible. As Fig. 1 shows, node x forwards a packet to the neighbor y because node y is closer to the base station. Greedy forwarding normally can lead a packet to the base station in dense networks, as the message originated from node x . However, there exist exceptions. As shown in Fig. 1, after node z receives a message from node g , it finds out that there is no closer neighbor to the base station to forward the message even though there exists a path. Thus, greedy forwarding fails at node z . Node z is called a concave node because it is the closest node to the base station in its local topology.

3.2. Cost-Based Forwarding

To treat the situations that greedy forwarding cannot handle, PAGER-M assigns a *cost* function to each sensor node using the location information of sensor nodes and the base station. For most sensor nodes, the costs equal to their Euclidean distances to the base station. For certain sensor nodes nearby concave nodes, the costs are higher than the corresponding geometric distances to the base station. When a packet reaches nodes close to concave nodes, instead of using greedy forwarding, it is forwarded following the high-cost-to-low-cost rule. There are two phases to establish the *cost* for each sensor. We describe the two phases in the following.

A. The Shadow-spread Phase

Let us consider the following process of shadow-spread algorithm on graphs shown in Fig. 3. In Fig. 3(a), node **A** is a concave node while nodes **B** and **C** are not. If we disconnect node **A** from the graph (shown in Fig. 3(b)), we can see that nodes **B** and **C** become concave nodes. We go one step further by disconnecting nodes **B** and **C** from the graph. As Fig. 3(c) shows, by disconnecting the sub-graph consisting of nodes **A**, **B** and **C** from the original graph, the resulting graph contains no concave node. Therefore, messages originated from the resulting graph in Fig. 3(c) will be forwarded to the base station using greedy forwarding without the danger of failure.

In the example shown in Fig. 3, we denote nodes **A**, **B** and **C** as *shadow* nodes, the rest of the nodes on the graph then become *bright* nodes. Specifically, the

bright nodes adjacent to shadow nodes are called *border nodes*, which on the graph shown in Fig. 3(a) are nodes **D** and **E**.

Differentiating nodes on the graph shown in Fig. 3 by their statuses (shadow/bright), we divide the original graph (Fig. 3(a)) into two sub-graphs. We call the sub-graph that contains shadow nodes (**A**, **B** and **C**) a *shadow area*. Similarly, the sub-graph that contains bright nodes is called a *bright area*. Further, as shown in Fig. 3, the void area on the graph that is encompassed by the concave node **A** is called a *partial partition*, which actually partially partitions the sensor network in Fig. 3 and creates concave node **A**.

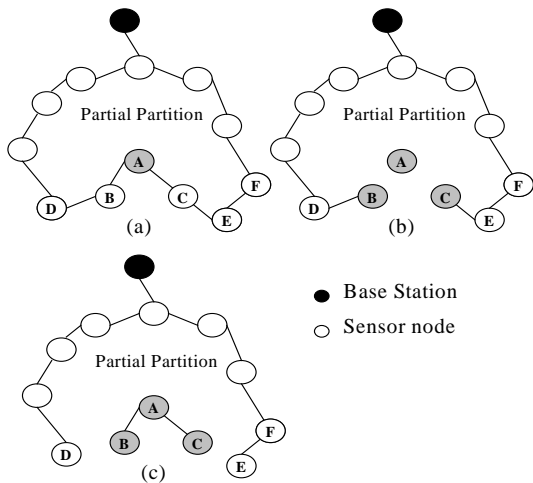


Fig. 3. An example process of the *shadow-spread*. (a) The graph contains concave node **A**. (b) After disconnecting node **A** from graph, new concave nodes **B** and **C** appear. (c) After excluding the sub-graph consisted by **A**, **B** and **C**, resulted graph contains no concave nodes.

In order to divide the original graph into shadow areas and bright areas as shown in Fig. 3(c), nodes should be able to exchange their status information (shadow/bright) along with their location information. This information exchange is realized by periodically broadcasting beacon messages that contain two fields: status and location. Every node on a graph should be able to get the location information of the base station. In our network model, sensor nodes receive the base station's location from its broadcast channel.

The distribution of shadow/bright areas of a sensor network depends on its topology and the communication range of sensor nodes. In Fig. 4 we give an example distribution of shadow/bright areas on a 200-node sensor network. Sensor nodes are randomly deployed on a $1000\text{ m} \times 1000\text{ m}$ sensing field with the base station located at (500, 1000). Each sensor node has a communication range of 113 meter, which creates a network topology with average degree of 8.

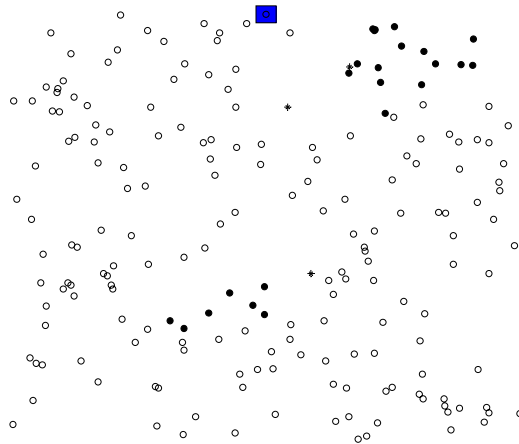


Fig. 4. Distribution of shadow/bright areas in a sensor network with 200 randomly placed sensor nodes. The base station is represented by the rectangle. Concave nodes are represented by “*”. Black nodes represent *shadow* nodes. White nodes represent *bright* nodes.

B. The Cost-spread Phase

Based on the sub-graphs resulted from first (shadow-spread) phase, the second (cost-spread) phase begins. To illustrate this phase, we show an example in Fig. 5. Initially each node on the graph has a variable equal to its physical distance to the destination. We mark the variables on each node. In the first step, every shadow node tries to avoid being surrounded by neighbors with larger variables. As Fig. 5(b) shows, node **A** finds that all its neighbors have larger variables. To avoid this situation, node **A** increases its variable to 22 to be larger than the maximum cost of its neighbors by Δ (Δ is set to 3 in this example). In the second step, nodes **B** and **C** find that all their neighbors have larger variable (since node **A** increased its variable). In response to this situation, they increase their variables to 23 and 25, respectively, as Fig. 5(c) shows. This process ends in the third step when node **A** increases its variable from 22 to 28, as shown in Fig. 5(d). Now, every shadow node (**A**, **B** and **C**) is satisfied because they can at least find a neighbor with a smaller variable. We denote the variable maintained in each node as the *cost*. If we give each node a forwarding direction to a neighbor following the high-cost-to-low-cost rule, as Fig. 5(e) shows, we establish paths across the whole graph to the base station.

To make the process shown in Fig. 5 possible, the cost information should be exchanged between nodes. Like status information used in the first (shadow-spread) phase, this is realized by adding the cost information to the periodically broadcasted beacon messages. We should notice that the process described above is limited in shadow areas instead of the whole network.

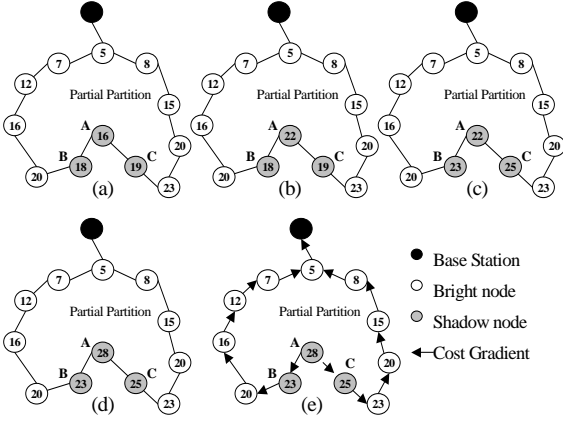


Fig. 5. An example process of *cost-spread* algorithm. (a) Before phase 2, shadow nodes (A, B, C) are determined. (b) Node A increases its cost to 22. (c) Node B and C increase their costs to 23 and 25 respectively. (d) Node A increases cost again to 28. (e) All shadow nodes (A, B and C) are satisfied with their costs; cost gradients are established from high-cost-to-low-cost.

3.3. Mobility Adaptability of Shadow Areas

In mobile sensor networks, shadow/bright areas can appear/disappear due to sensor node mobility. As Fig. 6(a) shows, initially node B is within the communication range of node A although these two nodes are moving apart; node A is not a concave node since its neighbor node B has a closer distance to the base station. After a period of time, as shown in Fig. 6(b), when node B has moved out of the communication range of node A, node B is no longer a neighbor of node A. Without node B as a neighbor, node A becomes a concave node. Then the shadow-spread and cost-spread processes begin. These processes finally result in shadow nodes (A, C and D) with different costs as shown in Fig. 6(b).

On the other hand, node mobility can also cause the disappearance of concave nodes and shadow areas. To explain this process, we consider the graph shown in Fig. 7. As Fig. 7(a) shows, initially nodes A and B are beyond each other's communication range although they are moving closer. Node A is hence a concave node because it is the closest node to the base station within its local topology. After a period of time as Fig. 7(b) shows, when nodes A and B are moving closer, they fall into each other's communication range. Then node A finds out that it is no longer a concave node because node B has a closer distance to the base station. After that node A first resets its cost to the Euclidean distance to the base station and changes its status to "bright". Then, it sends out beacon messages containing its new status (bright) to all its neighbors.

As Fig. 7(b) shows, this finally results in a graph without a shadow node. Because shadow areas can adaptively appear/disappear with the topology changes, PAGER-M has the self-reconfiguring feature.

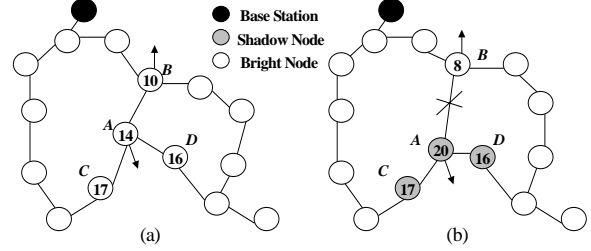


Fig. 6. Appearance of a shadow area. (a) No concave node and shadow area exist when node A and node B are within each other's communication range. (b) Link between node A and node B is broken due to movement, a new concave node and shadow area appears.

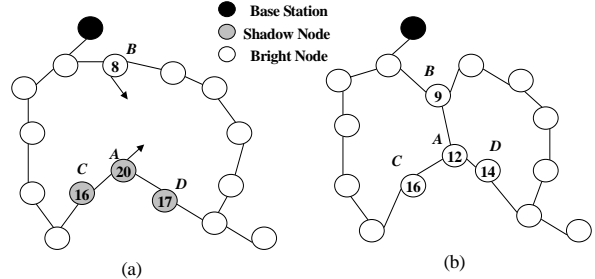


Fig. 7. Disappearance of a shadow area. (a) Node A and node B are moving approach to each other. (b) After the link established between node A and node B, node A is no longer a concave node.

4. Protocol Implementation

In our implementation of PAGER-M, we choose 802.11 MAC layer as the underlying MAC layer. In order to improve the performance of PAGER-M on 802.11 MAC layer, we have the following optimizations.

4.1 Beacon Message Broadcast Interval and Arrival Time

PAGER relies on periodically broadcasted beacons to provide nodes with their neighbors' location information. The performance is greatly affected by the choice of the beacon interval. In scenarios with high mobility, in order to have complete and up-to-date neighbor list, the beacon broadcast interval should be small. However, the performance of PAGER in mobile sensor networks can be seriously impaired if the beacon broadcasting is too frequent. There are two main reasons for the performance deterioration caused by beacon broadcast. First, beacon packets compete with data packets for the interface queue before they

are sent to the MAC layer. When the beacon broadcast interval is too small, the network interface queue is easily filled up because a large number of beacon packets are buffered. Therefore, new data packets from the routing layer will be dropped. Second, beacon packets contend with data packets for sharing the wireless media. This will cause high data packet loss ratio due to interference. In PAGER-M, we randomize and properly prolong the beacon broadcast interval to reduce the interferences caused by beacon packets.

On the other hand, longer the beacon broadcast interval, more out-of-date neighbor information contains in a sensor node's neighbor list. This may cause a node send out a data packet to a neighbor that has moved out of its communication range. To minimize the wrong forwarding decision caused by out-of-date neighbor information, the forwarding decision is made not only based on neighbors' costs but also the arrival time of a neighbor's beacon message. In PAGER-M, when a beacon message is received, the arrival time is recorded in the neighbor list with the beacon sender. When a sending node is choosing its neighbors to forward, not only the cost but also the arrival time of the neighbor is considered. For a node is forwarding messages at moment t , only neighbors whose beacon messages received at moment $t' > t - \tau$ are considered as forwarding candidates, where τ is a preset threshold.

4.2 Utilizing Path Redundancy

With proper density and arrival time threshold τ , multiple choices of forwarding neighbors may still available for a forwarding node following cost gradients. This provides redundancy for a sending node to choose an up-to-date neighbor to forward packets. We use this path redundancy to reduce the forwarding failure. In the example shown in Fig. 8, node **A** (with a cost 28) has three forwarding candidates (nodes **B**, **C** and **D**). How to choose the forwarding strategy among the forwarding candidate has impact on the performance of PAGER-M. For example, since nodes **B** and **C** have smaller cost than node **D**, if node **A** forwards a packet to nodes **B** or **C**, the packet will experience 7 hops before reaching the base station. Compared to the 8 hops path length via node **D**, choosing node **B** or **C** may be advantageous. However, as shown in Fig. 8, since nodes **B** and **C** are moving away from node **A**, packet forwarding may face transmission failure. Compared to nodes **B** and **C**, forwarding the packet to node **D** may be a "safer" choice although it increases the path length of the packet to the base station. In PAGER-M, the latter conservative forwarding strategy is adapted to reduce

the chance of transmission failure. This strategy is achieved by choosing the neighbor with closest arrival time within all available forwarding candidates (a forwarding candidate should has lower cost than the forwarding sensor node).

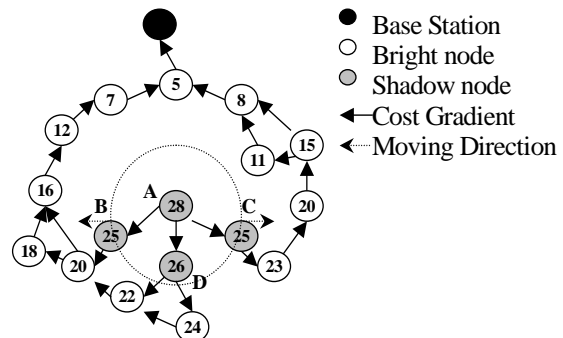


Fig. 8. Utilizing path redundancy to reduce transmission failure.

4.3 Interface Queue

Before packets from routing protocol are sent to the MAC layer, they are queued at the interface queue. If data packets have the same priority as beacon packets in the interface queue, both new-coming data packets and beacon packets will be abandoned when the queue length exceeds the limit. In order to improve the delivery ratio of data packets, we give data packets priority in the interface queue. When a data packet reaches the interface queue, it is inserted ahead of beacon packets that already in the queue rather than being buffered at the tail.

5. Performance Evaluation

We use the wireless extensions of ns-2 [25] developed by Carnegie Mellon University to implement our protocol. We use GPSR [18] and AODV [7] to compare with PAGER-M in mobile sensor networks. We choose AODV because we find that it performs better than Dynamic Source Routing (DSR) [4] in mobile sensor networks with a relatively large number of nodes (100~200 nodes). GPSR is chosen because it is a well-accepted stateless location-based routing protocol for mobile ad-hoc networks (including mobile sensor networks).

5.1. Simulation Parameters

Our simulation parameters are listed in Table 1. The base station is located at (500,1000). We simulate 100-node and 200-node sensor networks. In the 100-node case, we set the communication range to 178 m, which results in networks with average degree of 10. In the 200-node case, we constrain the average degree to 15

and 10 by setting the communication range to 155m and 126m, respectively. We simulate 8 CBR flows originated from 8 randomly chosen nodes across the whole networks. Each CBR flow is sent at 256 bps and uses 32-byte packets. Each sensor follows the random waypoint motion model to move randomly to a direction with a random speed uniformly selected from 0 m/s to 20 m/s. PAGER-M achieves its best delivery ratio when the beacon interval B ranges from 3 seconds to 7 seconds according to the average degree of sensor networks. In GPSR, the beacon interval B is set to 0.5~1 second to achieve its best delivery ratio.

Table 1. Simulation Parameters.

Number of nodes	100, 200
Workload	256bps \times 8
Simulation Length	100s
MAC Layer	802.11
Mobility Model	Waypoint
Maximum Speed	20 m/s
Sensing Field	1000 m \times 1000 m
Routing Protocol	GPSR, PAGER-M, AODV
Propagation Model	Two-Ray
Pause Time	0~40 seconds
Communication Range	178, 155, 126 m

We randomly generate 5 motion patterns for each scenario (different in pause time, maximum communication ranges, and number of nodes). Each motion pattern lasts 100 seconds. All experimental results are based on the average performance on these motion patterns.

In our simulations, the following metrics are evaluated: packet delivery ratio, path length, routing overhead and energy consumption.

5.2 Packet Delivery Ratio

The packet delivery ratio is measured as the ratio of the number of data packets delivered to the base station to the number of data packets sent by the source sensors. The packet delivery ratio is presented by the first set of figures (Figs. 9~11). We control the mobility of nodes by varying the pause time. In Fig. 9, we present the packet delivery ratio of protocols on 100-node sensor networks. PAGER-M achieves an average delivery ratio of $> 99\%$ with beacon interval 3~4 seconds, which is higher than those with the other two protocols.

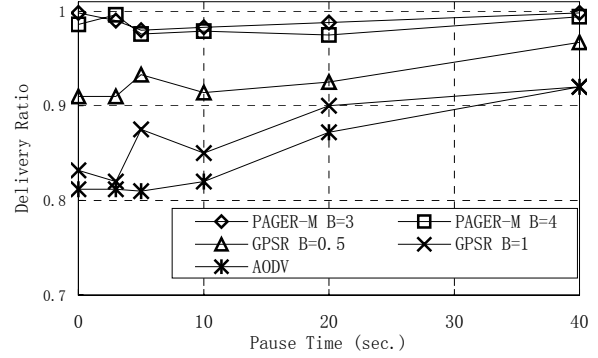


Fig. 9. Delivery ratio. Communication range=178 m, 100 nodes.

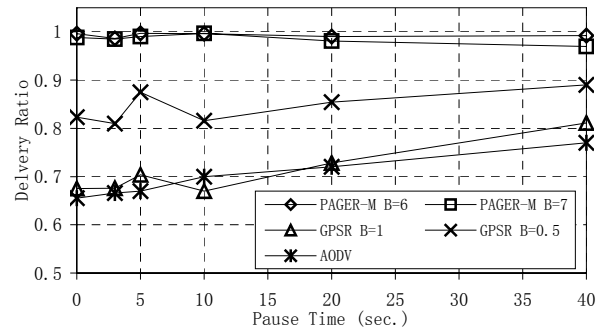


Fig. 10. Delivery ratio. Communication range=155m, 200 nodes.

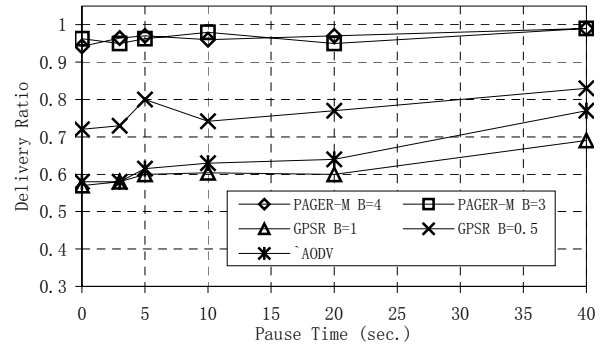


Fig. 11. Delivery ratio. Communication range=126 m, 200 nodes.

When we increase the number of nodes to 200, the delivery ratios of protocols are shown in Figs. 10~11. In Fig. 10, we set the communication range of sensor nodes to 155 m, which creates network topologies with average degree of 15. In Fig. 11, we reduce the communication range to 126 m, which results in network topologies with average degree of 10. In the communication range=155 m case, we set the beacon broadcast interval to 6~7 seconds. As we see in Fig. 10, the average delivery ratio of PAGER-M is about 99.3%, significantly higher than that of GPSR ($< 90\%$) and AODV ($< 80\%$). As we increase the beacon broadcast

interval of GPSR from 0.5 second to 1 second, as Fig. 10 shows, we observe significant decreasing of delivery ratio. This is because of GPSR's dependency on planarized graphs, which has high requirement of accuracy information of a sensor's local topology. When the communication range is shortened to 126 m, we set the beacon interval $B = 3\sim 4$ seconds in PAGER-M. As shown in Fig. 11, PAGER-M maintains an average delivery ratio of 96.6% while GPSR and AODV have average delivery ratios below 80% and 70%, respectively.

5.3. Path Length

The performance of average path length of the protocols is presented in Figs. 12~14 with different parameters. We present simulation results on 100-node networks with communication range=178 m in Fig. 12. We set the beacon interval of PAGER-M to 3~4 seconds in this case. The path length of AODV is about one hop more than the other two protocols. At the same time, the path lengths of PAGER-M and GPSR are quite close. Path length performance of these protocols on 200-node networks is presented in Figs. 13~14 with different communication ranges. When the communication range is 155m, as shown in Fig. 13, PAGER-M has an average path length in between those of GPSR and AODV. This is not surprising because of the conservative choice of forwarding destinations in PAGER-M (only beacon message senders received less than 3 seconds ago are considered as forwarding candidates). This conservative strategy makes a sending node choose not the neighbor closest to the base station but the "safest" one. As we decrease the communication range to 126m while increasing the beacon interval to 3~4 seconds in PAGER-M, as shown in Fig. 14, we observe that the average path length of PAGER-M increases to about 7. Again in this case, GPSR achieves the shortest path length compared to PAGER-M and AODV.

5.4. Routing Overhead

The routing overhead is measured in terms of control packets sent by the routing protocol. We present our experimental results in Fig. 15~17. We first present the 100-node network simulation results in Fig. 15 before introducing the 200-node case with different communication ranges in Figs. 16~17. In our simulations, the implicit beacon function of GPSR is disabled.

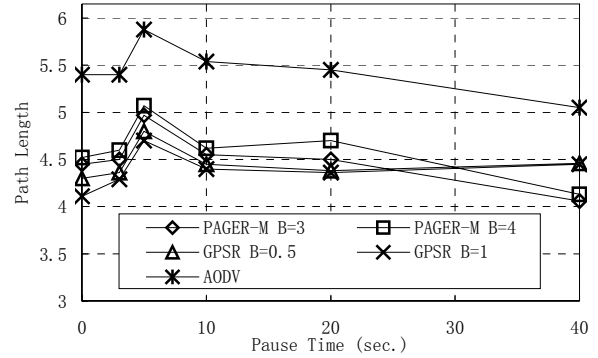


Fig. 12. Path length. Communication range=178m, 100 nodes.

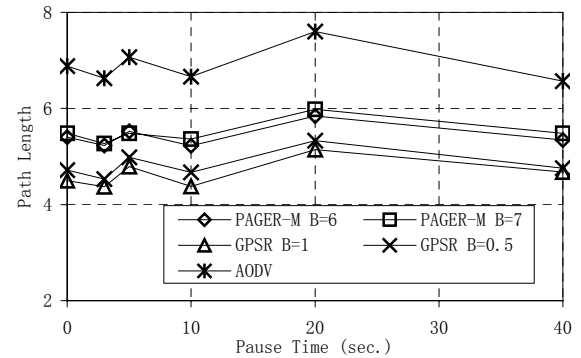


Fig. 13. Path length. Communication range=155m, 200 nodes.

In the 100-node networks, we set the beacon interval of PAGER-M to 3~4 seconds. As shown in Fig. 15, PAGER-M achieves lower routing overhead than the other two protocols because of its relatively long beacon interval. The 200-node networks cases are shown in Figs. 16~17. When we set the communication range to 155m as shown in Fig. 16, the routing overhead of PAGER-M is significantly lower than those of GPSR and AODV. Again this is due to the long beacon broadcast interval of PAGER-M, which reduces a bulk of the routing overhead in PAGER-M. The routing overhead of GPSR is more than twice than that of PAGER-M because of its short beacon interval. We also observe a decrease of the routing overhead in AODV with increasing pause time. This is because with reduced mobility, AODV sends out less routing packets to repair broken links. When the communication range is reduced to 126 m as shown in Fig. 17, in order to maintain the high delivery ratio, PAGER-M reduces beacon interval to 3~4 seconds, which causes the increasing of routing overhead to about 6500 and 8000, respectively. However, compared with GPSR and AODV, PAGER-M still has significantly less routing overhead.

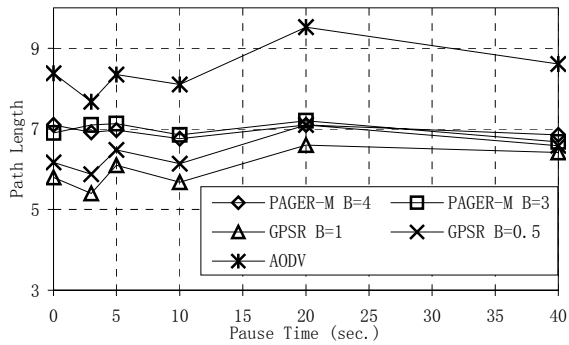


Fig. 14. Path length. Communication range=126m, 200 nodes.

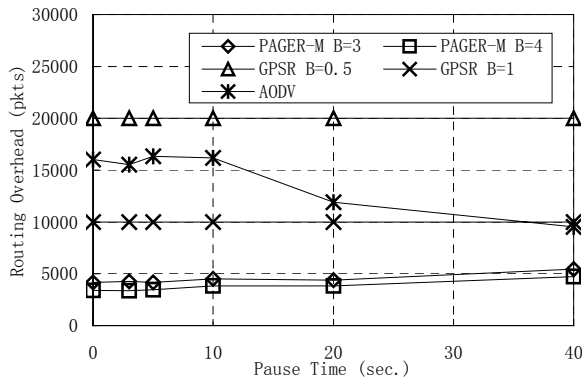


Fig. 15. Routing overhead. Communication range=178m, 100 nodes.

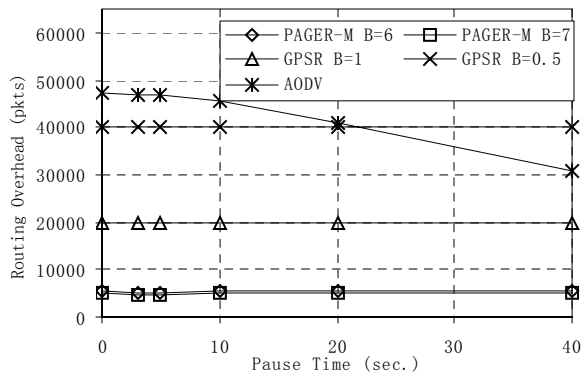


Fig. 16. Routing overhead. Communication range=155m, 200 nodes.

5.5. Energy Consumption

We simulate the 200-node networks to observe the energy consumption of PAGER-M. The performances are listed in Figs. 18~19. The energy efficiency of PAGER-M comes from its low control overhead and low path length as we shown previously. This energy efficiency of PAGER-M proves that PAGER-M is suitable for mobile sensor network.

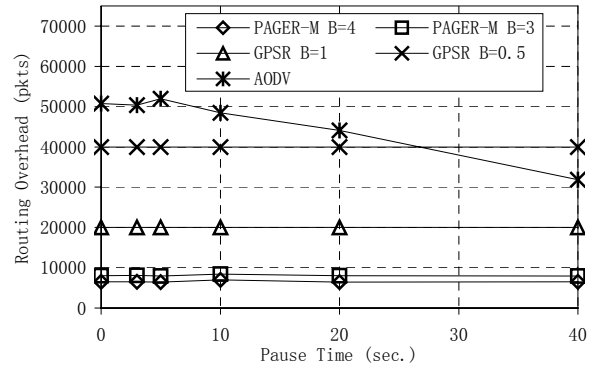


Fig. 17. Routing overhead. Communication range=126m, 200 nodes.

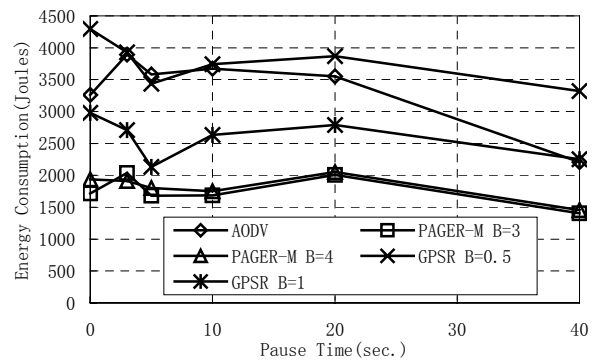


Fig. 17. Energy consumption. Communication range=126m, 200 nodes.

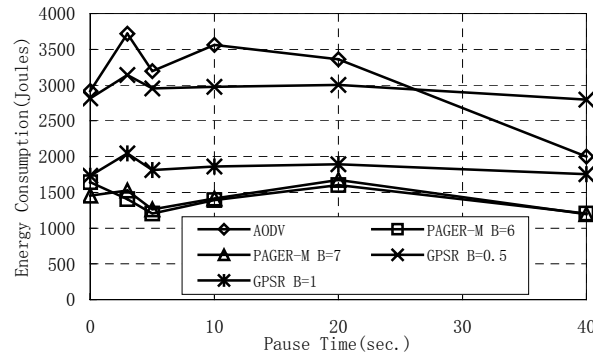


Fig. 17. Energy consumption. Communication range=155m, 200 nodes.

6. Related Work

In single-path/flooding method proposed by Stojmenovic et al. [14], when a concave node receives a message, it attempts to use flooding to send copies of messages to all its neighbors. By memorizing pass messages, the concave nodes can refuse receiving the same message again. The single-path/flooding method is proved to guarantee delivery, and the paths formed by this protocol are loop-free. Compared to their

scheme, PAGER-M uses single path strategy and does not require nodes to memorize past traffic.

Bose et al. and Karp et al. independently propose Greedy-Face-Greedy (GFG) [17] and Greedy Perimeter Stateless Routing (GPSR) [18] to handle situations that greedy forwarding fail. These two schemes are two quite similar routing schemes, which route packets around voids when concave nodes receive packets. GFG/GPSR do not require nodes to memorize past path/traffic and guarantee to find a path to the destination if there exists one. However, GFG/GPSR schemes require planarization of network topologies, which increases computational complexity in each sensor node and may cause partition in a connected network when topologies change frequently. Compared to GFG/GPSR algorithms, PAGER-M does not require planarization of network topologies. Further, PAGER-M does not route packets along voids but tries to route packets away from concave nodes before they get stuck.

SPEED [19] is a location-based routing protocol specifically designed for real-time applications. SPEED handles the situations that greedy forwarding fails by backpressure, which performs well in static sensor networks but is not sufficient to handle scenarios with high mobility.

Fang et al. [20] give a distributed algorithm to locate stuck nodes (local minimum). After locating stuck nodes, they presented a distributed algorithm to find out holes in sensor networks. By memorizing the shapes of holes in sensor networks, when a packet gets stuck in concave nodes, it computes the shorter side of a hole to reach the base station. Compared to GPSR, the scheme of Fang et al. does not require planarization of network topologies and can achieve shorter path lengths. However, when holes in sensor networks are large, communication overhead and memory consumption in nodes along holes are large. Further, the shapes of holes in sensor networks have to be updated frequently in scenarios with high mobility. Compared to the works by Fang et al. [20], PAGER-M does not require memorizing shapes of holes and can adapt to mobility rapidly.

7. Conclusion

In this paper, we presented a location-based routing protocol called PAGER-M that specifically designed for mobile sensor networks consisting of a large number of frequently moving sensor nodes. A cost function is assigned to each sensor node that has a value close to the Euclidean length of its shortest path to the base station. Greedy forwarding is used whenever possible. When a packet reaches sensor

nodes near local minimums, where greedy forwarding will be impossible after a number of hops, it is forwarded following high-cost-to-low-cost rule. In PAGER-M, multiple forwarding candidates are provided for a sending node. This path redundancy reduces the transmission failure. The beacon interval is prolonged and randomized to reduce interference and routing overhead. We compared the performance of PAGER-M, GPSR and AODV using extensive simulations. Experimental results show that PAGER-M has higher delivery ratio, lower routing overhead and lower energy consumption than GPSR and AODV.

References

- [1] I. Akyildiz, et al., "A Survey on Sensor Networks," *IEEE Communications Magazine*, Aug. 2002, pp. 102-114.
- [2] P. Juang, et al., "Energy-Efficient Computing for Wildlife Tracking: Design Tradeoffs and Early Experiences with ZebraNet," *the Tenth International Conference on Architectural Support for Programming Languages and Operating Systems*, Oct. 2002.
- [3] S. Cowen, S. Briest, and J. Dombrowski, "Underwater Docking of Autonomous Undersea Vehicles using Optical Terminal Guidance," *IEEE Oceans '97*, Halifax, NS, 6-9 Oct. 1997.
- [4] D. Johnson and D. Maltz, "Dynamic Source Routing in Ad Hoc Wireless Networks," *Mobile Computing Systems and Applications*, December 1994, pp. 158-163.
- [5] V. Park and M. Corson, "A Highly Adaptive Distributed Routing Algorithm for Mobile Wireless Networks," *Proceedings of INFOCOMM '97*, April 1997.
- [6] C. Perkins and P. Bhagwat, "Highly dynamic Destination-Sequenced Distance-Vector routing (DSDV) for mobile computers," *Proceedings of the SIGCOMM '94 Conference on Communications Architecture, Protocols and Applications*, August 1994, pp. 234-244.
- [7] C. Perkins and E. Royer, "Ad-Hoc On-Demand Distance Vector Routing," *Proceedings of the 2nd IEEE Workshop on Mobile Computing Systems and Applications*, February 1999.
- [8] J. Tateson and I. W. Marshall, "A Novel Mechanism for Routing in Highly Mobile Ad Hoc Sensor Networks," *EWSN 2004, LNCS 2920*, pp. 204-217, 2004.
- [9] W. Noh, K. Lim, J. Lee and S. An, "Time-Synchronized Neighbor Nodes Based Redundant Robust Routing (TSN3R3) for Mobile Sensor Networks," *EWSN 2004, LNCS 2920*, pp. 250-262, 2004.
- [10] W. R. Heinzelman, J. Kulik, and H. Balakrishnan, "Adaptive Protocols for Information Dissemination in Wireless Sensor Networks," in *Proc. ACM MobiCom '99*, Seattle, WA, 1999, pp. 174-85.
- [11] A. Manjeshwar and D. P. Agrawal, "TEEN: A Routing Protocol for Enhanced Efficiency in Wireless Sensor Networks," in *Proc. 15th Intl. Parallel and Distributed Processing Symposium*, pp. 2009 -2015, April 2001.

- [12] C. Intanagonwiwat et al., "Directed Diffusion for Wireless Sensor Networking," *IEEE/ACM Trans. Networking*, vol. 11, no. 1, Feb. 2003.
- [13] Z. Haas and M. Pearlman, "The Performance of Query Control Schemes for the Zone Routing Protocol," *IEEE/ACM Trans. Networking*, vol. 9, no.4, Aug. 2001.
- [14] I. Stojmenovic and X. Lin, "Loop-free Hybrid Single-Path/Flooding Routing Algorithms with Guaranteed Delivery for Wireless Networks," *IEEE Trans. Parallel Dist. Sys.*, vol. 12, no. 10, 2001, pp. 1023–32.
- [15] G. G. Finn, "Routing and Addressing Problems in Large Metropolitan-Scale Internetworks," ISI res. rep. ISU/RR-87-180, Mar. 1987.
- [16] E. Kranakis, H. Singh, and J. Urrutia, "Compass Routing on Geometric Networks," in *Proc. 11th Canadian Conf. Computational Geometry*, Aug. 1999.
- [17] P. Bose et al., "Routing with Guaranteed Delivery in Ad Hoc Wireless Networks," in *Proc. 3rd Int'l. Wksp. Discrete Algorithms Methods Mobile Comp. Commun.*, Seattle, WA, Aug. 20, 1999, pp. 48–55; also in *ACM/Kluwer WL Nets.*, vol. 7, no. 6, Nov. 2001, pp. 609–616.
- [18] B. Karp and H.T. Kung, "GPSR: Greedy Perimeter Stateless Routing for Wireless networks," in *Proc. 6th Annual International Conference on Mobile Computing and Networking (MobiCom 2000)*, 243-254.
- [19] T. He et al., "SPEED: A Stateless Protocol for Real-Time Communication in Sensor Networks," in *Proc. International Conference on Distributed Computing Systems (ICDCS2003)*, Providence, RI, May 2003.
- [20] Q. Fang, J. Gao, L. J. Guibas, "Locating and Bypassing Routing Holes in Sensor Networks", *IEEE INFOCOM'04*, March, 2004.
- [21] I. Stojmenovic, "Position-Based Routing in Ad Hoc Networks," *IEEE Commun. Mag.*, July 2002, pp. 128-134.
- [22] R. Jain, A. Puri, and R. Sengupta, "Geographical Routing Using Partial Information for Wireless Ad Hoc Networks," *IEEE Pers. Commun.*, Feb. 2001, pp. 48–57.
- [23] J. Li, J. Jannotti, D. De Couto, D. Karger, R. Morris, "A Scalable Location Service for Geographic Ad Hoc Routing," *Proc. IEEE/ACM Mobicom 2000*, pp. 120-30.
- [24] J. Hightower and G. Borriello, "Location Systems for Ubiquitous Computing," *IEEE Comp.*, Aug. 2001, pp. 57-66.
- [25] S. Bajaj, et al., "Improving simulation for network research," Technical Report 99-702b, University of Southern California, March 1999.